PORTABLE ABSOLUTE POSITION TRACKING SYSTEM FOR HUMAN HAND FINGERTIPS

M. Bezdicek[1], D. G. Caldwell[2]

(1) :
Ph.D. Student
Centre for Robotics and Automation
Newton Building
University of Salford
Manchester M5 4WT
Tel: *+44 (0)1612954010*
E-mail : *M.Bezdicek@pgr.salford.ac.uk*

(2) :

Italian Institute of Technology
(Instituto Italiano di Tecnolgia)
Via Morego
Genoa
Italy
E-mail: darwin.caldwell@iit.it

Abstract: There is absence of high precision truly portable human hand and fingertip trackers that are able to provide absolute position and motion data. Data of this format is vital to work in tele-robotics, VR and human performance assessment.

This paper will show the development of a new light weight, high precision and dedicated human hand magnetic tracking system. It will be shown that this magnetic tracker has distinct benefits compared to other tracking techniques. The tracker presented is smaller then any other hand tracking system currently reported and moreover provides absolute fingertip tracking in all six degrees of freedom with absolute accuracy of 0.2 mm. The paper will describe the operation of the device which is based on near magnetic field coupling and consists of one transmitter antenna triad and six receiver antenna triads. The transmitter and receiver antennas triads are enclosed in a cubical casing. The base transmitter station is mounted on the dorsal surface of the hand and the receivers are mounted on the fingertips and any arm point to be tracked. The tracker is completely battery powered and has complete wireless compatibility with the Bluetooth wireless specification. Use of the Bluetooth standard, ensures that the tracker can have a cable-free connection to computers, PDAs or other electronic equipment.

Key words: tracker, magnetic, portable, hand, fingertip.

1- Introduction

The human hand and fingers form an integrated assembly that constitute the most dexterous part of the human body. A hand has at least 27 degrees of movement [4], [16], seven for the thumb, four for each of the fingers, two for palm arch and two for wrist motion. This advanced and complex kinematic format gives dexterity, combined with delicacy of movement and capacity for power grasping, and endows humans with incredible powers of manoeuvrability and capability for interaction through various object grasping and manipulation strategies. At the same time the hand and fingers also have a sensory function fundamental to these exploring purposes.

Most industrial robots have only up to 6 DOF [2] in the full arm motion and little dexterity in the grip function.

Within the rapidly developing VR world there is a hunt for alternative computer input devices able to give users complex and more natural interaction than those currently provided by a keyboard or mouse. The capacity to use the complexity of the human hand in a natural and intuitive manner forms one important train of research in this domain. There are various tasks where hand motion tracking is required [15], [17], [18]. For example

i) in movies when computer generated characters are involved,

ii) for artists and computer aided sculpturing,
iii) for hand exercises - rehabilitation, for gaming and so on [8].
iv) Control of a teleoperated anthropomorphic robotic hand [4], [19].

While the accuracy and fidelity of the motion of hand and finger tracking are important in all these applications, for a robotic hand the control accuracy of fingertips position is particularly critical since any mismatch between the location of the user joints and the robot joints could result in a unwanted (and real) physical collision. Current input gloves are unable to satisfy these accuracy requirements, because of way the finger position is sensed.

Clearly there is a great opportunity for the development of a new hand tracking system for use in robot hand control and indeed all other areas. For robotic telepresence such a tracker should provide all six coordinates (3 positions and 3 rotations) of every fingertip relative to palm. These coordinates can be subsequently be converted in to direct finger joint angles for known dimensions of the robotic hand [5].

It is of course, obvious that a generic robotic hand will have different dimensions to those of an operator. This will result in errors in the mapping from the operator to the robotic hand typical when using traditional input glove technology [6]. With a direct fingertip tracking technique it is obvious, that positions of the fingertips of the robotic hand will have exactly same configuration as the operator's fingertips (although the exact joint angles need not be exactly equal). For example distance between a thumb fingertip and index fingertip will be exactly same on the robotic and also on the operator's hand. This grasping point position matching forms the basic premise to enable the use of the robotic hand for precise fine manipulations [3] – eg picking up the pen, write and act as well as larger grasping and power grip manoeuvres.

A further aspect of the use of accurate fingertip sensing is that this methodology can be used for very high fidelity calibration of conventional gloved systems. There are many factors that affect the accuracy of these gloves and complicate their use including; different users hand sizes, palm and joints geometry, sweating of the hand if glove on, sensor accuracy and linearity problems, etc. For more serious tasks calibration is always necessary [20]. Compared to work, where authors [7], [11], [12] have been using directly joint angles to calibrate glove without knowing actual fingertips positions, the presented tracking system can accurately provide missing information about fingertips position and make calibration of gloved systems much easier, with much higher degree of accuracy. Direct fingertip tracking brings new extension for gloves calibration from accuracy and flexibility point of view.

This paper presents the design of a new dedicated human hand tracking system based on magnetic techniques that is able to provide the coordinates of fingertips with a high degree of accuracy. The tracker accepts data from six sensors providing six degrees of freedom for each of sensor (Figure 5). All together there are $6 \cdot 6 = 36$ DOF for the whole tracker (five sensors on fingertips and one mounted on arm). This 36 DOF actually gives more information than is required for tracking of the human hand (27 DOF) does, which is particularly useful for precise hand motion mapping. The range of the tracking space has the form of a hemisphere with a radius of 200 mm. The tracker is based on AC magnetic field coupling between a set of three orthogonal transmitting coils and a set of three orthogonal receiving coils (Figure 3). Accuracy of tracking is 0.2 mm. This tracker is small and portable because is generating only weak magnetic field which can be sensed only in short distance (up to 200 mm from transmitter). Communication is via a wireless Bluetooth link.

This paper will describe the hardware design of the whole tracker and followed by a detailed description of the system software involving DSP program description. The paper will conclude by looking at the main applications and future development issues.

2- Hardware of the hand tracker

Design of a tracker based on magnetic field coupling is a very delicate task which requires precise components and fast signal processing. PCB design is also critical. The tracker developed in this work consists of single digital signal processor (DSP) and set of additional components chosen with respect to portability and battery power requirements. The heart of the hand tracker is a DSP from Texas Instruments, TMS320F2810 clocked at 150 MHz [25]. The DSP generates signals, which

are after amplification used for driving the orthogonal transmitter coils to excite the magnetic fields. Moreover the DSP is also in conditioning the return signal and estimating the positions and orientations of the sensors.

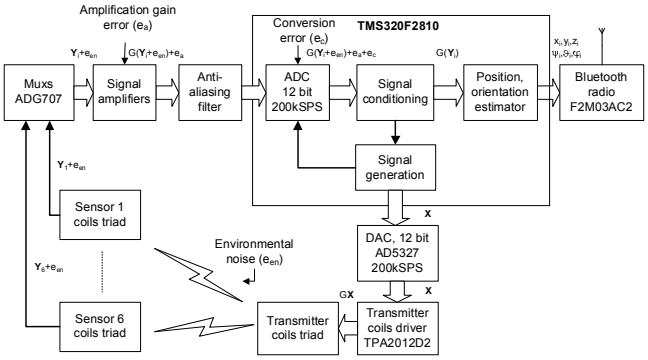

Figure 1: Block diagram of the magnetic hand tracker.

The block diagram of the hand tracker is shown in figure 1.

The magnetic field is excited by a transmitting antenna triad with the drive signal for these transmitter antennas being generated by the DSP. However, since the DSP doesn't have an integrated DAC alternative options must be pursued including
i). an integrated PWM generator, which can produce a sine wave output [26] or
ii). an external 12-bit DAC.

To ensure higher quality output signals the external 12-bit DAC was selected. A power amplifier follows after the DAC to amplify the signal to create measurable magnetic fields in the field of motion of the fingertips. The power amplifier is a D-class amplifier with minimal temperature looses and a compact package well suited for portable devices. The transmitter's antenna triad has three orthogonal transmitting coils forming a cube with each side 12 mm long.

Since the magnetic field is producing very low induced voltages in the sensor coils it is also necessary to amplify the return signal. A two stage differential amplifier has been selected to amplify the signals. The differential input amplifier is built from two independent operational amplifiers, which are combined with low-pass and anti-aliasing filters. Differential and common mode filtering is applied at the inputs to the amplifier by a simple filter circuit consisting of passive components. A differential filter with a roll-off at 36.1 kHz was used. Common mode filtering was applied at the much higher frequency of 330 KHz to avoid compromising the CMRR of the amplifier.

To boost the signal levels resonant circuits are used. The resonant circuit radically alters the impedance of the circuit at the tuned frequency, which is good for boosting the signal and moreover for increasing immunity against noise. The signal used in the tracker has a constant frequency of 12 kHz.

As might be expected the production of the coil and the determination of the coil parameters are critical. Unfortunately, there is no supplier who offers commercially produced coil triads with required features, i.e. three coils that must be orthogonally wound on a non-magnetic core (Figure 3). For this reason coils have extensive configuration testing the coils were made in-house. The coils need to have precise geometry, exactly same value of induction, yet must be as small as possible.

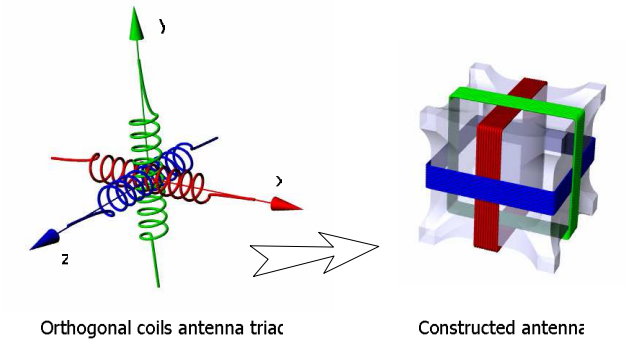

Figure 3: Orthogonal coils antenna for transmitter/receiver.

To achieve these requirements a compromise has been made. The final transmitter is a Perspex cube with side 12 mm, 50 turns of 0.11 m diameter copper wire. The sensor is also made from a Perspex cube with 9 mm sides and 300 turns of 0.04 mm copper wire (Figure 4). Every single coil is specially calibrated, tested and the correction coefficients acquired are applied in DSP code.

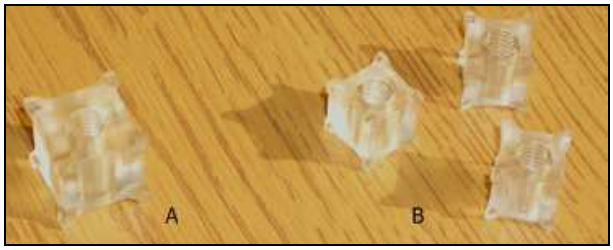

Figure 4: Coils cores: A) 12 mm transmitter triad core, B) 9 mm receiver triad cores.

Mounting a sensor on the hand is a complicated task, because of different hand sizes, skin stretching and aspect of conformability. Five sensors are mounted on the fingertips to track the fingers and one is mounted on the arm for wrist motion sensing (Figure 5). The transmitter antenna is mounted on the dorsal surface of the palm. Fingertips sensors are clamped on finger by small easily detachable clip.

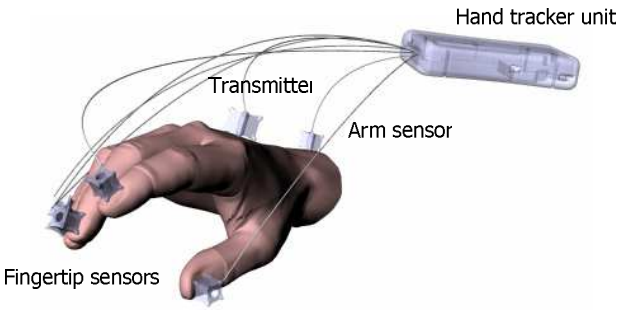

Figure 5: Coils placement on the hand.

The tracker is powered by one 1000 mAh Li-ion battery, which provides energy for at least three hours of continuous operation. Charging of the battery takes about four hours and the tracker can be used during the charging as normal.

3- Description of software for magnetic tracker

The target of the DSP code is to excite orthogonal magnetic field, at the same time extract quantities representing the magnetic field vectors in the sensor's coils and then estimate position and orientation from them.

The code for the DSP has been written in C++ in the Code Composer Studio 3.1. As already mentioned the DSP device chosen for this application runs at a maximum CPU frequency of 150 MHz and supports real-time debugging through a JTAG interface, which is very handy and can do the task much faster and easier [23]. The DSP is capable of generating reference signal for the transmitter coils, conditioning the return signal and estimating sensors coordinates in real time.

Figure 6 shows signals for one sensor coordinates evaluation. This consists of three stage excitation and of capturing induced voltages in the sensor. There is a phase shift between the transmitted reference signal and the return signals; however this is easily compensated with a software demodulator.

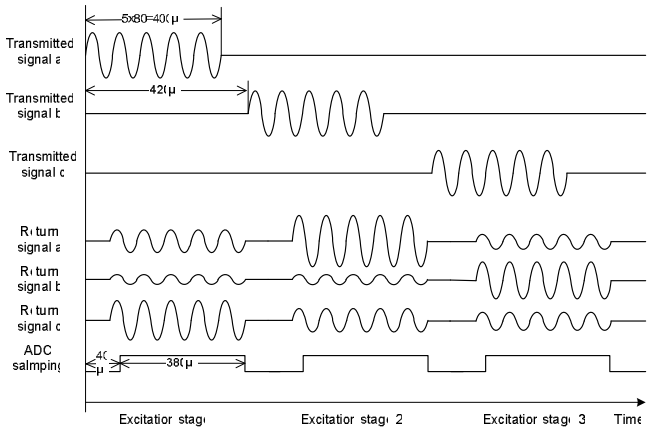

Figure 6: Tracker signal timing diagram for one sensor measurement.

The block diagram of the low level signal conditioning displayed inside the DSP block on figure 1 is shown in detail in figure 7.

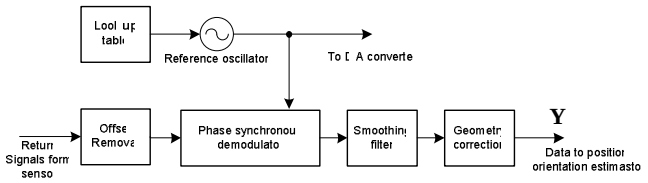

Figure 7: Low level signal conditioning block diagram.

The sinusoidal reference signal has a frequency of 12 kHz and is generated using a software look-up table with an arbitrary 16 points per period, giving a required signal update rate of 200 kSPS. The DAC sampling is triggered by an interrupt at 200 kHz. This gives a relatively high sample rate compared with the oscillator frequency and relaxes the constraints on the anti-aliasing filter. The DSP running at the maximum CPU clock speed of 150 MHz executes 750 cycles between consecutive interrupts of frequency 200 kHz, all the following conditioning code has to be completed in this time.

The offset removal algorithm removes any DC offset component which may be present on the input signal and would disrupt correct operation of the demodulator. It works by maintaining a running average of the input signal and subtracting the result from each input reading. Since the average value of a sine wave is zero over a complete number of cycles, only the DC offset component remains after averaging and this can be subtracted from the ADC reading on a point-by-point basis, effectively AC coupling the input signal [22].

As figure 7 shows the second stage of the conditioning chain comprises a demodulator, which is synchronised to the reference oscillator to determine the phase shift of the return signal and yield a full-wave rectified sine wave of the appropriate polarity. The use of a digital technique to produce the reference oscillator means that the reference signal is readily available, and this permits a simple demodulation technique to be used which is insensitive to phase shift. The return signal can be thought of as a complex vector, the real and imaginary parts of which can be computed independently by multiplying with the two quadrature components [21]. The magnitude of the vector is computed from the root of the sum of the squares of these components. The determination of phase is based on the result of an 'exclusive OR' between the sign of the reference oscillator and that of the return signal: if these signals are in phase the signs should be the same and the result is false, if the signals are in anti-phase the signs are opposed and the result will be true. Phase was determined using a 'majority vote' based on the previous 16 results (i.e., over one complete oscillator cycle). This technique was found to give good results near the null point, where the signal-to-noise ratio is low [24].

The third stage of the signal conditioning process is the smoothing filter, which smoothes the rectified signal magnitude into a smooth and stable digital result. The smoothing is necessary due to the presence of magnetic field distortion in the air surrounding the system. A simple moving average filter was constructed using a window over whole excitation step. The filter runs on a point-by-point basis: each data point from the output of the demodulator is added to a circular buffer, and the average computed by subtracting the oldest value from a running total, adding the newest value, and scaling.

The final stage of the signal conditioning consists of measurement sensors geometry correction. Fixed offset and gain adjustments are applied, and the result is used to index into a correction map to retrieve a correction in bits which is added to the reading.

Once nine measured voltages from the sensor and their signs are known the matrix $\mathbf{Y}$ representing the induced voltages in the coils can be composed:

$$\mathbf{Y} = \begin{bmatrix} a_1 & a_2 & a_3 \\ b_1 & b_2 & b_3 \\ c_1 & c_2 & c_3 \end{bmatrix}, \quad (1)$$

From the matrix $\mathbf{Y}$ position and orientation can be estimated.

The technique for evaluating position and rotation of the magnetic tracker is described in detail in [1], [10], [14] and involves the following processes.

The near magnetic field produced by circular loop antenna can be described in terms of radial and tangential components, as shown in figure 8.

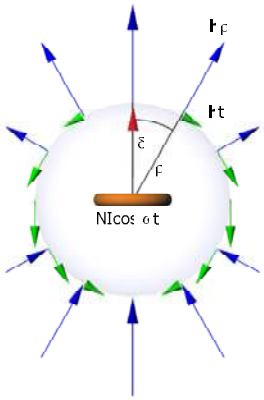

Figure 8: Simplified representation of magnetic field for current carrying closed loop.

The loop shown in figure 8 is excited with a current $i(t) = I\cos\omega t$. The magnetic field produced at a point of distance ρ and off axis angle δ is described completely by radial and tangential components:

$$H_\rho = \frac{M}{2\pi\rho^3}\cos\delta, \quad (2)$$

$$H_t = \frac{M}{4\pi\rho^3}\sin\delta, \quad (3)$$

where $M = NIA$ is scaled magnetic moment of the loop, and A and N represents the area and number of turns of the loop [8]. The sensor loop antenna responds only to the field component aligned with the loop orientation vector (perpendicular to the plane of the loop). Measurements of the three orthogonal transmitted signals from ground antennas as received by the set of three orthogonal receiving antennas produce information which is sufficient to determine six position and

orientation parameters. This assumes orientation and position parameters are independently determined. To synthesise a position-orientation algorithm, coordinates and a vector-matrix formulation relating sensor output to source excitation must be defined. The geometric relationship between a three-axis source and a three axis sensor is shown in figure 9.

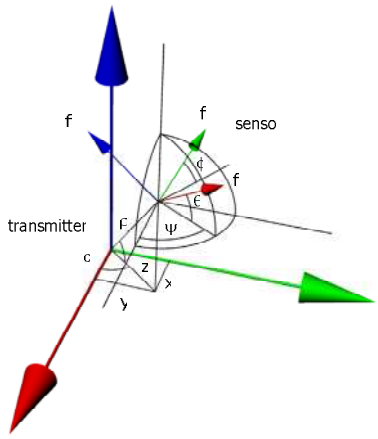

Figure 9: Geometric relationship between a three-axis source and a three axis sensor

From the geometrical definition shown in figure 9 and equations (2), (3) a five step estimation algorithm can be composed.

The position and orientation algorithm consists of these steps:

1. Measure the coupling between transmitter and receiver (Figure 6), to obtain the matrix $\mathbf{Y}$ and filter it.
2. Compute the orientation invariant matrix $\mathbf{D}^2 = 1/C^2\mathbf{Y}^T\mathbf{Y}$, where C is gain constant.
3. Estimate the positions x, y, z from $\mathbf{D}^2$.
4. Compute $\mathbf{D}^{-1} = \left(\mathbf{D}^2\right)^{\frac{1}{2}}$.
5. Estimated the orientation matrix $\mathbf{A} = 1/C\mathbf{Y}\mathbf{D}^{-1}\mathbf{T}_C$, where $\mathbf{T}_C$ is the compensation rotation matrix.
6. Estimate the orientation angles ψ, θ, ϕ from matrix $\mathbf{A}$.

As can be seen all six coordinates are available at the output from the algorithm. This calculation must be repeated for all six sensors.

The previously determined position and orientation of sensors relative to the transmitter needs to be transmitted to any PC or other piece of electronic equipment (Figure 10). This can be done through a wireless Bluetooth link. The Free2Move Bluetooth class 2 (10 m range) module is used. The tracker can work in endpoint or connecting Bluetooth mode. The endpoint mode basically means, that the tracker is configured as a slave and another device, which is in connecting mode has to establish communication with it. When the tracker is configured in the connecting mode it is able to perform a search for surrounding devices and connect to an appropriate one.

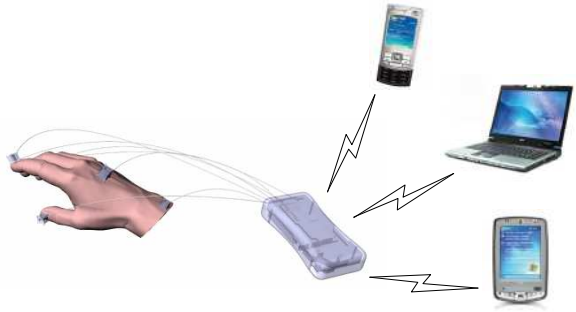

Figure 10: Hand tracker Bluetooth connection possibilities.

Bluetooth communication isn't only used for sending the sensor's coordinates. It is also used for tracker configuration and set up. Records of coordinates may have a different form dependant on how many sensors are in use, what precision is required and whether other features like timestamps are turned on.

4- Conclusion

Wireless hand tracker was developed (Figure 11). The tracker has six sensors operating in the range +/-200 mm. A number of tests have been conducted to determine the device accuracy. For testing the industrial robot RR K-1607IHP with special setup has been used. Results show that static accuracy for position is better than 0.2 mm and orientation is better than 0.1 deg. The tracker reading resolution is 0.05 mm within 100 mm distance form transmitter (Table 1).

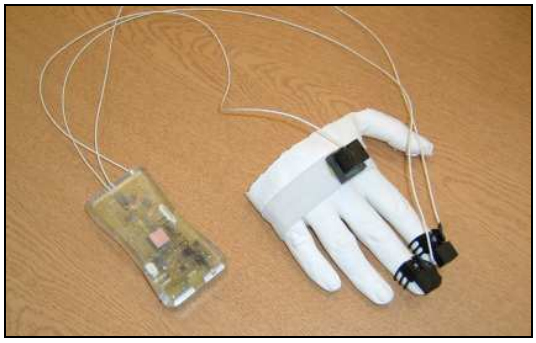

Figure 11: Hand tracker prototype.

Several applications have been developed for the hand tracker demonstration: 3D flying bugs test application, VR hand test application and keyboard simulator (Figure 12).

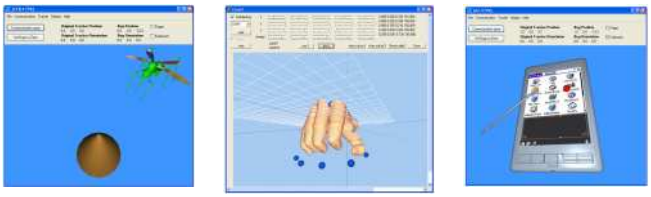

Figure 12: Examples of developed testing applications (3D bug test app., VR hand, keyboard sim.).

The 3D flying bugs application is just for tracker visualisation and calibration, allows user to see coordinates of all sensors.

The VR hand test application is dedicated for fingertips position mapping onto the hand. An inverse kinematics problem must be solved for every finger to determine finger joint angles. This application is still under development.

The keyboard simulator is application focused on VR simulation of handheld devices like PDA, mobile phone and act. From experience with data gloves we realized that information from the gloves has limited accuracy even for mobile phone interaction. As proved; using of fingertip hand tracker is providing good foundation for this kind on simulation.

Number of sensors	1+6
Number of DOF	6 per sensor
Operating range	+/- 200 mm hemisphere
Static accuracy	Pos. 0.2 mm, rot. 0.1 °
Resolution	0.05 mm / 100 mm
Update rate	140 records per second for whole hand
Communication	Wireless - Bluetooth 10 m range
Box dimensions	104 x 51 x 21 mm
Weight including battery and coils	170 g
Battery type	Li-ion 3.6 V, 1000 mAh
Battery operation time	3 hours

Table 1: Hand tracker specifications.

5- Future work

There are some points on the tracker which should be improved. First there will be work to make the coils smaller. As next the algorithm for estimation of coordinates will be improvement for compensation due metallic objects and influence of noise. Some work has already started on UI based techniques to map data from the tracker on to joint angles with focus on robotic hand control and for data glove calibration. In future development of 3D applications for the tracker will be done.

6- References

[1] Bezdicek, M., "Precise human hand tracking and motion mapping onto robot using UI methods", PhD thesis draft, 2006

[2] Corke, P.I., "A Robotics Toolbox for Matlab", IEEE Robotics and Automation Magazine, pp.24-32, also at www, 1996

[3] Craig, J., "Introduction to Robotics: Mechanics and Control", Addison-Wesley 1989, ISBN: 0201095289

[4] Chua, P.Y., "Tele-Operated High Speed Anthropomorphic Dextrous Hands with Object Shape and Texture Identification", IROS 2006, Beijing, November 2006 (accepted)

[5] Denavit, J., Hartenberg, R. S.: "Kinematic Notation for Lower Pair Mechanisms, Based on Matrices", ASME J. of Applied Mechanics 6/1955, S. 215-221

[6] Grepl, R., "Kinematics and Dynamics of Mechatronics Systems", Study support material, Brno 2005, Czech Republic

[7] Griffin, W.B., Findley, R.P., Turner, M.L., Cutkosky, M.R., "Calibration and Mapping of a Human Hand for Dexterous Telemanipulation", ASME IMECE 2000 Conference, 2000

[8] Kay, S.E., "Handbook of Virtual Environment Technology", Lawrence Erlbaum Associates, 2002

[9] Marchese, S.S., Buckley, M.A, Valleggi, R. and Johnson, G.R. "An optimised Design of an active orthosis for the shouder - an iterative approach", ICRR, Stanford CA, 1997

[10] Raab, F.H., Burlington, V., "Remote object position and orientation locater", US patent 4314251, 1982

[11] Rohling, R.N., Hollerbach, J.M., "Calibrating the Human Hand for Haptic Interfaces," Presence, vol. 2 no. 4, pp. 281-296, 1993

[12] Turner, M.L., Findley, R.P., Griffin, W.B., Cutkosky, M.R., Gomez, D.H., 2000, "Development and Testing of a Telemanipulation System with Arm and Hand Motion", ASME IMECE Symp. on Haptic Interfaces, 2000

[13] Vukobratovic, M., "Introduction to Robotics", Springer, Berlin, Heidelberg New York 1989

[14] Werner, H.E., "Helmet-mounted sighting system", US patent 4287809, 1981

[15] Ascension Technology Corporation, http://www.ascension-tech.com, internet page, 2006
[16] Gray's Anatomy of the Human Body, http://education.yahoo.com/reference/gray/, internet page, 2006
[17] Polhemus Fastrak, http://www.polhemus.com/fastrak.htm, internet page, 2006
[18] Smart Technology tactile displays, http://www.smarttec.co.uk, internet page, 2006
[19] The Shadow Dexterous Hand, http://www.shadowrobot.com, internet page, 2006
[20] Bezdicek, M., Brown, S.: "Wireless CyberGlove interface unit", project report, Salford University, UK, 2004
[21] Texas Instruments: Download C28x IQMath Library - A Virtual Floating Point Engine (SPRC087), 2004
[22] Herceg, E., E.: "Handbook of Measurement and Control", Schaevitz Engineering, 2002
[23] Spectrum Digital: eZdsp F2812 Technical Reference, 2004
[24] Szczyrbak, J., Schmidt, E., D., D.: "LVDT Signal conditioning Techniques", Lucas Varity, 2005
[25] Texas Instruments: TMS320F2810, TMS320F2812 Digital Signal Processors (SPRS174), 2004
[26] Texas Instruments: Using PWM Output as a Digital-to-Analogue Converter on a TMS320C240 DSP. (SPRA490), 2004